Evaluation of the mechanical properties and degree of conversion of 3D printed splint material

Leila Perea-Lowery[1], Mona Gibreel[1], Pekka K. Vallittu[1,2], Lippo Lassila[1]

[1]Department of Biomaterials Science and Turku Clinical Biomaterials Centre-TCBC, Institute of Dentistry, University of Turku, Finland. Address: Itäinen Pitkäkatu 4B (2nd floor), FI-20520, Turku, Finland

[2]City of Turku Welfare Division, Oral Health Care, Finland. Address: Lemminkäisenkatu 2, FI-20520, Turku, Finland

Corresponding author

Leila Perea-Lowery

leiper@utu.fi

Abstract

Objective: To evaluate the effect of post-curing method, printing layer thickness, and water storage on the mechanical properties and degree of conversion of a light-curing methacrylate based resin material (IMPRIMO® LC Splint), used for the fabrication of 3D printed occlusal splints and surgical guides.

Methods: 96 bar-shaped specimens were 3D printed (Asiga MAX), half of them with a layer thickness of 100 µm (Group A), and half with 50 µm (Group B). Each group was divided in three subgroups based on the post-curing method used: post-curing with light emitting diode (LED) and nitrogen gas; post-curing with only LED; and non-post-curing. Half of the specimens from each subgroup were water-stored for 30 days while the other half was dry-stored (n=8). Flexural strength and flexural modulus were evaluated. Additional specimens were prepared and divided in the same way for surface hardness (n=96), fracture toughness, and work of fracture (n=96). Five specimens were selected from each subgroup for evaluating the degree of conversion (DC). Data were collected and statistically analyzed with 1-way, 2-way ANOVA, and Tukey post-hoc analysis (α=0.05).

Results: The 2-way ANOVA showed that the post-curing method and water storage significantly affected the investigated mechanical properties (P<0.001). The 1-way ANOVA revealed a statistically significant difference among the tested groups on the investigated properties (P<0.001). After water storage, the 100 µm subgroup post-cured with only LED showed higher flexural strength (51±9) than the 50 µm and 100 µm subgroups that were post-cured with LED in addition to nitrogen gas atmosphere (38 ±5, 30 ±3) ($p < 0.05$). The 50 µm subgroup post-cured with only LED showed the highest significant flexural modulus values (1.7 ±0.08) ($p < 0.05$). However, the 50µm subgroup post-cured with LED plus nitrogen showed significantly higher surface hardness values ($p < 0.05$) among the investigated groups. The non-post-cured subgroups showed the lowest values, which were significantly different from the other subgroups ($p<0.05$).

Conclusion: The post-curing method, water storage, and printing layer thickness play a role in the mechanical properties of the investigated 3D Printed occlusal splints material. The combination of heat and light within the post-curing unit can enhance the mechanical properties and degree of conversion of 3D printed occlusal splints. Flexural strength and surface hardness can increase when decreasing printing layer thickness.

1. Introduction

Occlusal stabilization splints (SS) are devices often used in the treatment of temporomandibular disorders (TMDs), which is a term used to describe masticatory muscle weakness and pain of temporomandibular joints and associated structures.[1] The use of such SS for the treatment of TMDs and bruxism is clinically accepted and has a low risk of side effects.[2,3] Occlusal splints reduce the muscular tension and protect teeth against wear by distributing occlusal forces generated during teeth grinding and/or jaw clenching.[4]

Autopolymerizing or heat-cured polymethyl methacrylate (PMMA) has been used for the fabrication of hard SS.[5] The fabrication is made on plaster casts poured from an intraoral impression of the patients' dental arches. Then, intra-oral try in and adjustments are carried out in order to obtain the desired adaptation to the teeth. However, the process is time-consuming for the dentist and the patient. Furthermore, the quality and clinical performance of SS are affected by pore formation, large amount of residual monomer content and shrinkage which may occur during the production process.[6]

Additive manufacturing (AM) has been used as an alternative for the fabrication of three-dimensional (3D) resin-based SS. The functioning of AM technologies involves the use of two-dimensional data (2D), which is acquired from the segmenting process of 3D models produced via computer-aided designing (CAD) and computer-aided manufacturing (CAM) systems to physically replicate 3D objects in a layer-by-layer method.[7–10]

This technique is more time-efficient compared with the traditional manufacturing method, which also results in accurate occlusal splints.[11,12] It is associated with less processing complications, which happen due to technical errors and/or material properties such as polymerization shrinkage. Accurate shape and thickness of the stent can be obtained. Additionally, the occluding contact points can be optimized with the aid of a virtual articulator and glide paths of lateral and protrusive movements.[13,14]

For manufacturing occlusal SS, the use of 3D printing equipment might then be a cost-effective alternative to obtain precise 3D occlusal splints. The production of a digital and subsequent physical splint lead to a precise planning of the treatment sequence, time saving and more predictable results.[15] A variety of 3D printing methods and devices are currently available. Based on the printing methods, the current printing systems may be categorized as a) extrusion printing, where a material is handed out from a nozzle with computer controlled movement of a 3-axis stage; [16] b) inkjet printing, where droplets of an ink are allocated using 3-axis stages;[17] c) laser melting and sintering, where the high temperature of the laser is utilized to sinter specific regions in a powder bed while a platform moves up or down and the material is coupled layer-by-layer generating a 3D structure;[18] and d) stereolithography printing (SLA), which uses photopolymers that are kept in a Z-axis controlled vat, resulting in a 3D printed structure due to the direct exposition of the polymer to light.[19]

A digital scanner is used for capturing the three-dimensional image of the structure and creating a CAD file, which is then processed, edited and transformed into a stereolithography (STL) file. This STL file can be used as the input for an STL apparatus. Then, inside the apparatus, the structure is made by using any of the currently available printing methods. Two irradiation methods are involved in SLA printing, which are mask irradiation and direct irradiation. In the first method, each layer of a polymer is solidified using UV radiation that is produced by a lamp and transmitted through a mask with transparent areas equivalent to the section of the model to be fabricated. [20] Vector photo fabrication is the second irradiation method used in SLA printing. In this method a laser is involved for polymerizing each layer of the polymer defining the cross section of the 3D object. This direct irradiation system is conformed by a vat containing a photosensitive polymer, a mobile platform where the model is built, a laser irradiating UV light and an optical system for the laser to be directed along the polymeric layer. [10]

In the SLA printing process unpolymerized resin is removed by rinsing the 3D printed object with solvent and placing it in an ultraviolet light oven in order to accomplish final polymerization.[21–23] Since resins used for 3D printing purpose usually contain ultraviolet absorbers, translucent objects can be obtained such as implant drilling guide and transparent surgical models.[24] Casts with high accuracy can be obtained if such printing is combined with imaging data like cone beam computed tomography.[25]

Although it is known that 3D printed resin materials are anisotropic in relation to the printing direction,[26] literature concerning the evaluation of the mechanical properties[11] and wear resistance[27,28] of 3D printed occlusal devices is generally scarce. Therefore, the aim of this study was to investigate the effect of post-curing methods, printing layer thickness, and water storage on the mechanical properties and the degree of conversion of a light-curing methacrylate based resin material (IMPRIMO® LC Splint), used for the fabrication of 3D printed occlusal splints and surgical guides.

2. Materials and methods:

2.1 Flexural strength and flexural modulus testing:

In this study, a methacrylate-based acrylic resin (IMPRIMO® LC Splint, SCHEU-DENTAL GmbH, Iserlohn, Germany) was evaluated, which is a light-curing resin (bisphenol-A-ethoxylate diacrylate (Bis-EMA), structural formula shown in Figure 1) used for the manufacture of high-precision 3D printed occlusal splints and surgical guides.

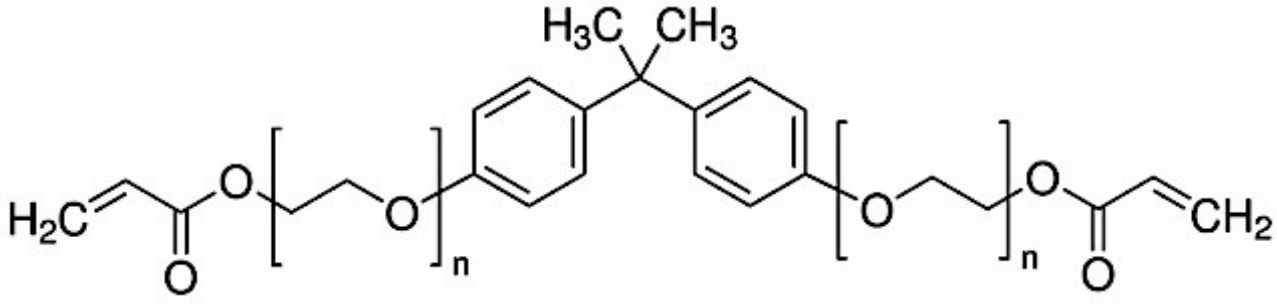

Figure 1. Structural formula of the major monomer component (bisphenol-A-ethoxylate diacrylate) of the resin system

Bis-EMA is the ethoxylated version of Bis-GMA, which has a higher molecular weight (MW=540 g/mol) that can be reduced by the strong secondary molecular interactions given by hydroxyl groups, allowing for higher degree of double bond conversion (DC) and better mechanical properties to be achieved. [29] Photo-polymerization is done by means of image projection systems. For flexural strength and flexural modulus testing, 96 bar-shaped specimens (3.2×10.0×65.0 mm) were printed in a horizontal direction with digital light printing (DLP) 3D printer (ASIGA MAX™, SCHEU-DENTAL GmbH, Iserlohn, Germany). Half of the specimens (n=48) was printed with a layer thickness of 50 µm (Group A), and the other half (n=48) with 100 µm layer thickness (Group B).

The 3D printed specimens were cleaned from fluid resin residues by placing them for three minutes in an ultrasonic cleaning unit containing a cleaning liquid (IMPRIMO® Cleaning Liquid, SCHEU-DENTAL GmbH, Iserlohn, Germany), which is a water-based cleaning agent. Subsequently, the specimens were rinsed with isopropanol for three minutes in a different cleaning unit (Form Wash, Formlabs, Berlin, Germany). Afterwards, group A was divided into three equal subgroups (n=16/subgroup) according to the post curing method used as follow: **Scheu oven 50 µm**, where specimens were polymerized in a light oven with light emitting diode (LED) exposure technology and protective gas device (nitrogen gas atmosphere) to avoid the formation of an

inhibition layer for three minutes (IMPRIMO® Cure, SCHEU-DENTAL GmbH, Iserlohn, Germany) at a wave length of 365-405 nm and a pressure of 1.8 bar; **Form Cure 50 µm**, where the specimens were polymerized in a light curing unit with LED at wave length of 405 nm for 30 minutes at 60 °C (Form cure, Formlabs, Berlin, Germany); and **non-post-cured 50 µm**, where the specimens were not exposed to any post-curing mechanism. Group B specimens were divided into three subgroups following the same parameters as per group A. For each subgroup, half of the specimens was stored in distilled water at 37° C for 30 days while the other half was dry stored under ambient laboratory conditions (23 ± 1 °C) before testing.

The flexural strength and flexural modulus were assessed by conducting a 3-point bending test for the printed specimens in air at room temperature using a universal testing machine (Model LRX; Lloyds Instruments Ltd, Hampshire, UK). The speed of the crosshead was adjusted to be 5 mm/min and the distance between the supports of the test specimens was 50 mm.

2.2 Surface microhardness

The same procedures described above were repeated to obtain additional bar-shaped specimens (4 × 10 × 10 mm) for surface hardness measurement (n=16/subgroup). A Vickers hardness testing machine (Duramin-5, Struers, Ballerup, Denmark) was used for conducting the surface microhardness test on selected portions of the printed specimens. The force used was 490.6mN for 15s.

2.3 Fracture toughness (K_{ic}) and work of fracture (Wf)

Ninety-six 3D printed bar-shaped specimens (4.0 × 8.0 × 40.0 mm) that were divided in the same manner as described above were used for the purpose of performing fracture toughness testing. It was evaluated using single-edge notched bend (SENB) specimens. The printed specimens were placed on a flat holder and then centrally notched with a 0.15 mm double-sided diamond disk

(Komet, Brassler, Legmo, Germany). The notches were polished and sharpened by a straight edged razor blade. The length of the notch was 3.0 mm. The specimens were exposed to a 3-point bending test with a universal testing machine at a cross head speed of 1.0 mm/min and the distance between the supports of the test specimens was 32 mm. After testing, the crack length (a) was calculated as the average of 3 measurements of the notch length on the fracture surface of each specimen with light microscope (Leica; Leica Microsystem, Wetzlar, Germany).The K_{Ic}[30] was calculated in MPa $m^{0.5}$ using the following equation:

$K_{Ic=}$ [P L/B $W^{3/2}$] f(x),

f (x)=$3x^{1/2}$ [1.99-x (1-x) (2.15-3.95x+$2.7x^2$)/(2 (1+2x)(1-x) $^{3/2}$ and 0<x<1 with x=a/W

where *P* is the maximum load (in Newton) and *L* is the span distance in millimeters (mm), B is the specimen thickness in mm, W is the specimen width, x is a geometric function dependent on a/W and a is the crack length in mm. Then, the SENB specimens were used for determining the total fracture work (W_f) [31] in J/m^2, by using the equation:

Wf = U/ [2 B (H − a)] 1000

2.4 Degree of double bond conversion (DC)

Five specimens were selected from each subgroup and the degree of double bond conversion (DC) was measured. The unpolymerized material was considered as the control for measuring the DC of methyl methacrylate (MMA) to PMMA. DC was analyzed using Fourier Transform Infrared (FTIR) spectrometer (Frontier FT-IR spectrometer, Perkin Elmer, Llantrisant, UK). Five specimens from each subgroup, as well as the nonpolymerized material were analyzed. Each polymerized test specimen was ground with a file and the resulting powder was placed on the ATR crystal for the

test. DC was measured by evaluating the absorbance peak intensity of aromatic bonds around at 1608 cm^{-1} wave number on the FTIR spectrum. Absorbance peak intensity values 1608 cm^{-1} wave numbers for unpolymerized and polymerized specimens were proportioned and DC values were recorded as percentage (%) using the following equation:

DC % = 100* (1- cured aromatic absorbance peak intensity/uncured aromatic absorbance peak intensity).

All data for the evaluated properties were collected and statistically analyzed with 1-way analysis of variance (ANOVA) followed by Tukey multiple comparison post hoc analysis using a statistical software (IBM SPSS Statistics v21, IBM, Redmond, WA, USA). Multi-way ANOVA was conducted to detect the effect of post-polymerization method, printing layer thickness, and water storage as the independent variables on the evaluated properties (α=0.05).

3. Results

The 2-way ANOVA statistical analysis showed that the post-curing method and the water storage significantly affected the values of the investigated mechanical properties (P<0.001). Printing layer thickness did not have a significant effect on the fracture toughness, work of fracture, and the degree of conversion (P=0.088, P=0.179, P=0.412) while it affected significantly the other investigated properties (P<0.05) as shown in Table 1. A significant interaction exists between the layer thickness and post-curing method (P=0.003).

Table 1. *P* values of two-way and 3-way ANOVA for the evaluated mechanical properties

Variable	Flexural strength (*P* value)	Flexural modulus (*P* value)	Work of fracture (*P* value)	Hardness (P value)	Fracture toughness	Degree of conversion (P value)
Post –polymerization method	**< 0.001**	**< 0.001**	**< 0.001**	**< 0.001**	**< 0.001**	**< 0.001**
Layer thickness	**0.032**	**0.001**	**0.179**	**0.007**	**0.088**	**0.412**

Storage	**< 0.001**	**< 0.001**	**< 0.001**	**< 0.001**	**< 0.001**	**-------**

P<.05 significant

The mean values for flexural strength, flexural modulus, fracture toughness, work of fracture, and micro hardness of the tested groups are presented in Table 2.

Table 2. Mean values of evaluated mechanical properties of tested groups

Group	Subgroup	Storage	Flexural strength (MPa) Mean ± SD	Flexural modulus (GPa) Mean ± SD	Work of fracture (J/m^2) Mean ± SD	Fracture toughness (MPa $m^{1/2}$) Mean ± SD	Vickers hardness Mean ± SD
Group A (50 µm)	**Scheu**	**Water**	38±5^{ac}	1.1 ±0.1^{ab}	97 ±15^{ab}	0.7 ±0.1^{abd}	16.4 ±1.1^{a}
		Dry	53 ±6^{fgh}	1.3±0.2^{bf}	139 ±12^{c}	0.8 ±0.1^{abc}	17.7 ±1.6^{af}
	Form Cure	**Water**	48 ±8^{cf}	1.7 ±0.1^{h}	129±25^{bc}	0.6 ±0.1^{ad}	13.5 ±0.8^{be}
		Dry	63 ±11^{h}	1.5 ±0.1^{gh}	127 ±12^{bc}	0.8±0.1^{c}	13.8 ±0.8^{b}
	Non-post-cured	**Water**	14 ±0.6^{de}	0.2 ±0.1^{e}	370 ±24^{f}	0.3 ±0.1^{ef}	2 ±0.3^{c}
		Dry	22 ± 0.8^{bd}	0.5 ±0.1^{d}	285 ±8^{e}	0.4 ±0.1^{e}	11.1 ±0.6^{d}
Group B (100 µm)	**Scheu**	**Water**	30 ±3^{ab}	0.9 ±0.1^{c}	180 ±18^{d}	0.7 ±0.1^{abd}	12.2 ±0.8^{de}
		Dry	45 ±6^{cf}	1.1 ±0.1^{ac}	125 ±10^{bc}	0.7 ±0.1^{bc}	17.1 ±0.7^{af}
	Form Cure	**Water**	51 ±9^{fg}	1.2 ±0.3^{ab}	71 ±18^{a}	0.6 ±0.1^{d}	12 ±0.9^{d}
		Dry	60 ±10^{gh}	1.4 ±0.2^{fg}	123 ±13^{bc}	0.8 ±0.1^{c}	17.9 ±0.8^{f}

	Non-post-cured	**Water**	11 ±0.5^{e}	0.2 ±0.1^{e}	396 ±42^{f}	0.3 ±0.1^{f}	2.2 ±0.6^{c}
		Dry	16 ±0.6^{de}	0.3 ±0.1^{de}	257 ±13^{e}	0.3 ±0.1^{ef}	11.1 ±0.7^{d}
P value			**<0.001**	**<0.001**	**<0.001**	**<0.001**	**<0.001**

SD, standard deviation.
P<.05 significant
Same superscripted lowercase letters indicate groups not statistically significantly different when compared by Tukey multiple comparisons post hoc analysis (*P*>.05).
Same superscripted uppercase letters indicate groups not statistically significantly different when compared by one-way ANOVA analysis (*P*>.05).

The DC % for the tested groups is presented in Figure 2. Figure 3 represents the IR spectra showing the peaks used for calculating the DC%.

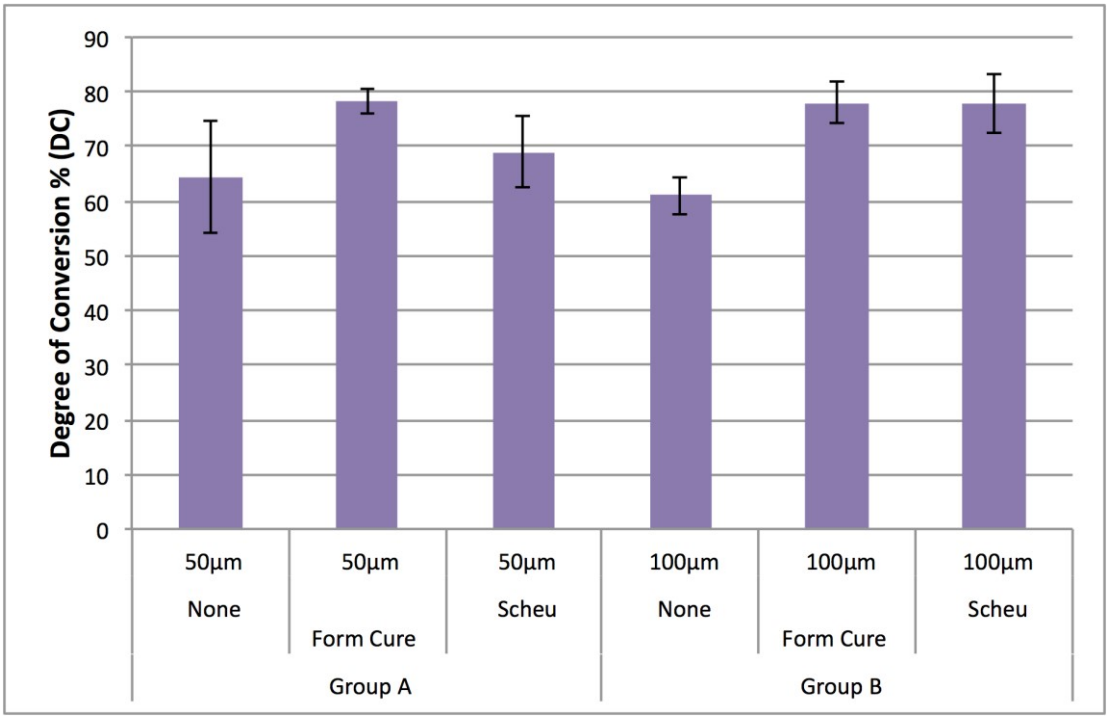

Figure 2. Diagram of degrees of double bond conversion % for the tested groups

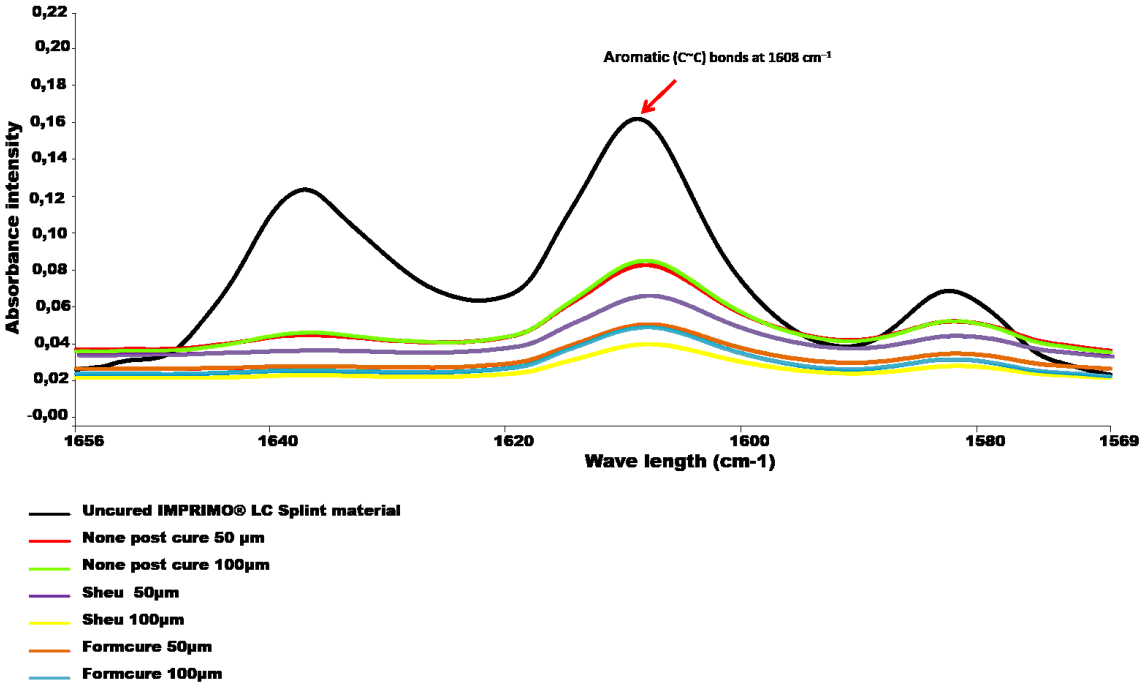

Figure 3. IR spectra showing the Aromatic bond peak (red arrow) used for calculating the DC%

The 1-way ANOVA revealed a statistically significant difference on the flexural strength (Figure 4), flexural modulus, fracture toughness (Figure 5), work of fracture, Vickers micro hardness (Figure 6), and DC percentage values among the tested groups (P<0.001).

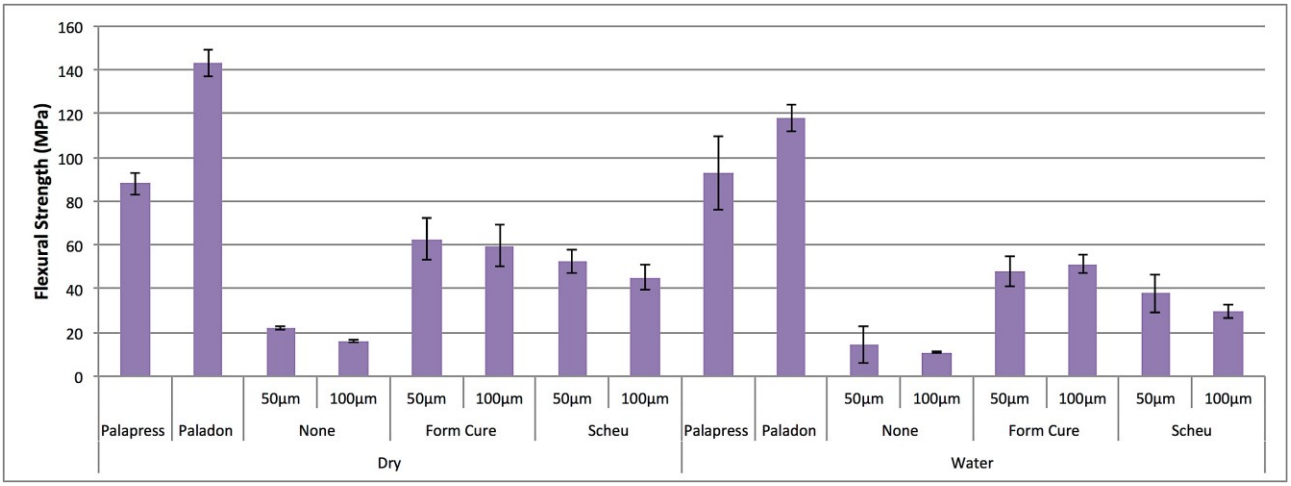

Figure 4. The flexural strength (MPa) according to post-curing method, printing layer thickness and storage conditions

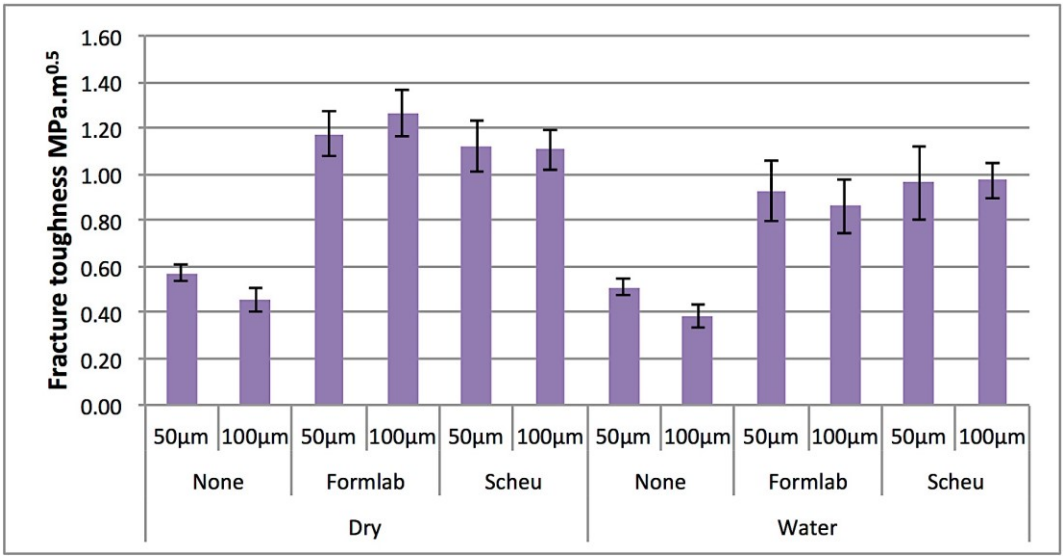

Figure 5. The fracture toughness (Mpa.m0.5) according to post-curing method, printing layer thickness and storage conditions

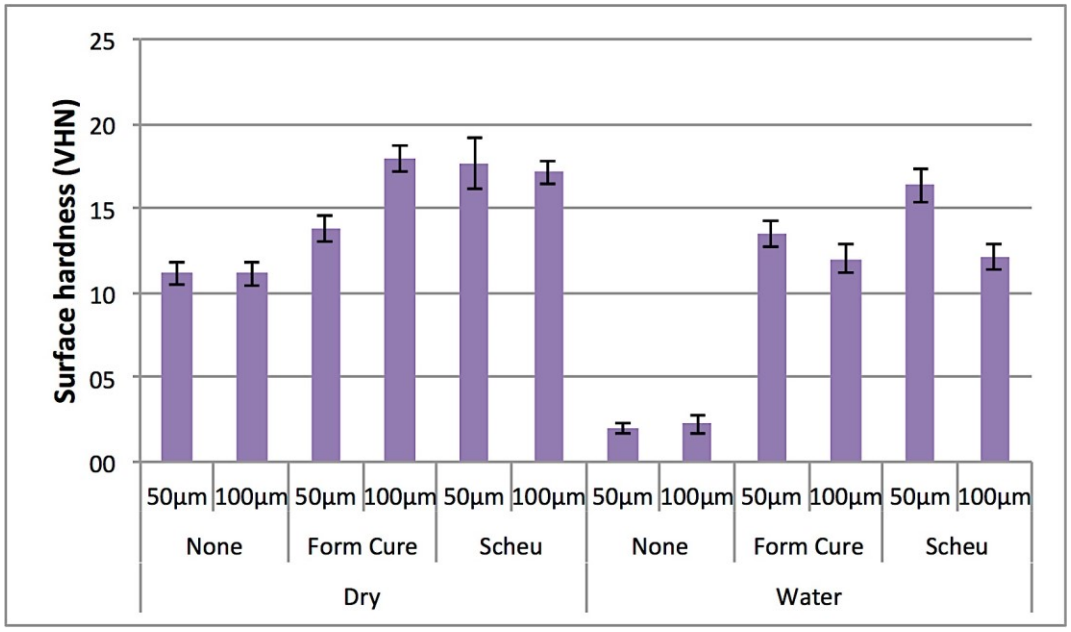

Figure 6. The surface hardness (VHN) according to post-curing method, printing layer thickness and storage conditions

The obtained flexural strength values were compared with those for clear autopolymerizing and heat-polymerizing acrylic resin materials (Palapress; Kulzer GmbH and Paladon 65; Kulzer GmbH respectively) tested in a previous study[32] as shown in Figure 4.

For dry specimens, the mean flexural strength values of Scheu oven 50 µm, Form Cure 50 µm, and Form Cure 100 µm subgroups were not significantly different from each other (P=0.055). After water storage for the 30 days, the flexural strength values of Form Cure 50 µm and Form cure 100 µm subgroups were significantly the highest (P<0.05) while being not significantly different from each other (P=0.438). The highest significant flexural modulus values of dry specimens were recorded by Form Cure 50 µm, and Form Cure 100 µm subgroups, while after water storage only Form Cure 50 µm subgroup showed the highest significant values (P<0.001) followed by Scheu oven 50 µm, and Form Cure 100 µm subgroups which were not significantly different (P=0.534). A graphical representation of the load-deflection values according to post-

curing method for 50μm and 100μm printing layer thickness is shown in Figure 7 and 8 respectively.

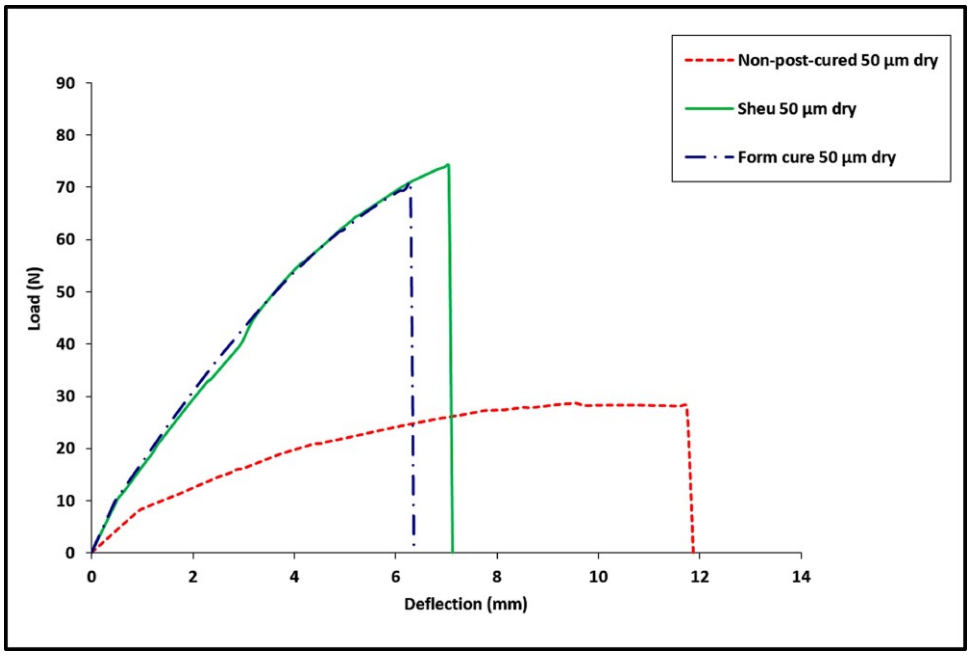

Figure 7. The load-deflection curves according to post-curing method for 50μm printing layer thickness

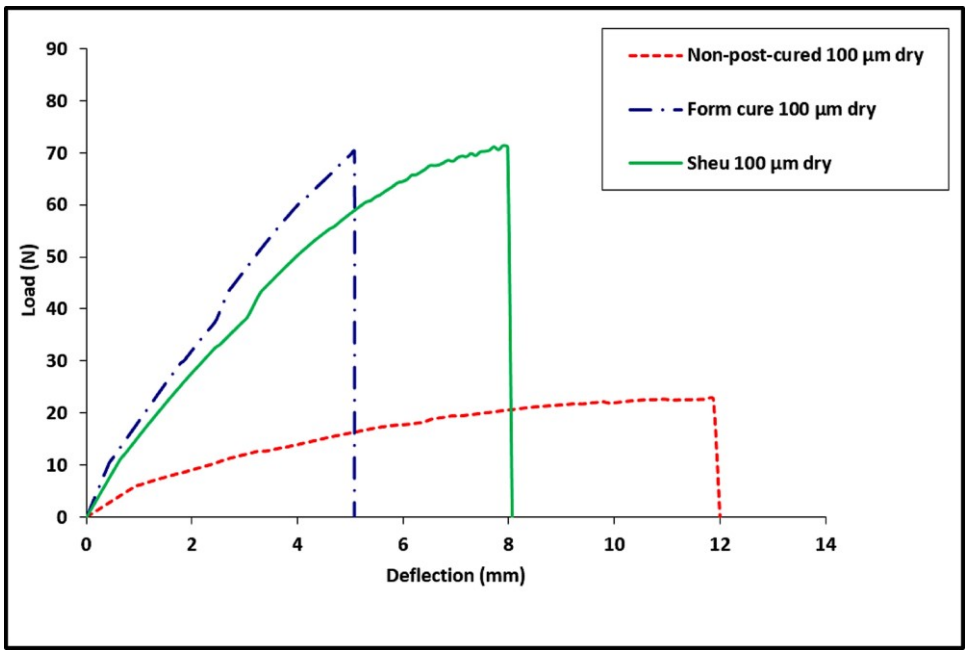

Figure 8. The load-deflection curves according to post-curing method for 100μm printing layer thickness

The non-post-cured 50 µm and non-post-cured 100 µm subgroups recorded the lowest significant flexural strength, modulus, fracture toughness, and surface hardness in both groups under dry and water storage (P<0.001).

Regarding fracture toughness under dry storage conditions, Scheu oven 50 µm, Form Cure 50 µm, and Form Cure 100 µm subgroups were not significantly different (P=0.256), while after water storage a non-significant difference was found among Scheu oven 50 µm, Scheu oven 100 µm, and Form Cure 50 µm subgroups (P=0.067).

Water storage decreased significantly the surface hardness values of all tested subgroups except for the Scheu oven 50 µm subgroup (P>0.05). Surface hardness values for the water stored specimens of Scheu oven 50 µm subgroup followed by those of the Form Cure 50 µm subgroup were significantly higher than the other tested subgroups (P<0.001). The highest significant values for the work of fracture was recorded by the non-post-cured 50 µm and non-post-cured 100 µm subgroups especially the water-stored specimens (P<0.001). Regarding the DC%, Scheu oven 50 µm, Scheu oven 100 µm, Form Cure 50 µm, Form Cure 100 µm recorded the highest values and were not significantly different from each other (P=0.164).

4. Discussion

This study demonstrated the effect of polymerization methods, printed layer thickness, and water storage on the mechanical properties and the degree of double bond conversion of LC Splint, which is a material used for manufacturing 3D printed devices used as occlusal splints and surgical guides. The overall results demonstrated a significant difference between post-cured and non-post-cured specimens.

This study was conducted isothermally at 37° C in agreement with previous studies[28,33] since occlusal splints are not exposed to temperature changes intraorally as they are

usually inserted in the patients' mouth at night when there is no intake of hot and cold food or drinks. Post-curing is essential to provide high conversion for photopolymers used in 3D printing and to obtain superior mechanical properties.[34] It is achieved by either additional light exposure and/or heating up the photopolymers. Previous investigations showed that different post-curing methods result in variable shrinkage strains and mechanical properties.[35,36] In case of bruxism treatment, occlusal splints are used for longer durations and exposed to higher load values up to 770 N.[37] Therefore, identifying the mechanical properties of the material after complete curing is necessary for evaluating whether such 3D printed material is suitable or not for using in the fabrication of occlusal devices.

The degree of polymerization and curing depth of photoresins are affected by many parameters such as the characteristic of light curing unit,[38,39] layer thickness,[22] exposure duration,[38] and distance between light source and the cured material,[40] temperature and curing time.[40] When choosing the correct printing layer thickness, an over curing effect should be avoided. This occurs during the manufacturing process when the printer's light penetrates deeper into the object than the specific layer thickness, [41] which leads to inaccuracies in the 3D printed object. Additionally, it leads to a heat development during polymerization that impairs the conversion of the single print layers.[42]

Since 3D printing resins for DLP printers must be properly photopolymerized layer by layer to form the objects, they must have a low viscosity during the printing process. In this study, Bis-EMA was used, where the absence of the hydroxyl group decreases its viscosity and makes the monomer a good candidate for 3D printing.[43] A previous study showed that decreasing the thickness of the printed layer increases the flexural strength of the 3D printed splints by increasing the number of different layers and bonding.[28] Additionally, the extent of polymer curing plays a role in the surface hardness of photopolymers.[38,40,44,45] This was in agreement with our study where the flexural modulus and hardness values for the post-cured specimens with 50 μm printing layer

thickness were significantly higher than those printed with 100 µm layer thickness. This could be attributed to the decrease in light intensity when it passes through a bulk of resin material due to its absorption and scattering by resin particles causing a gradation of curing from top surface inward.[46]

Increasing the degree of monomer conversion enhances the photopolymers' strength and decreases their elongation at break.[34,36] The DC is also crucial for medical resin-based devices since it has a high impact on their biocompatibility.[47] Additionally, the material's composition seems to be more relevant for its toxicity than DC.[47] Nevertheless, a high DC in a material prevents the release of its residual monomers,[48] and promotes its physical and mechanical properties.[49] Increasing the resin temperature decreases its viscosity and allows better movement of free radicals and development of polymer chains resulting in better monomer conversion rate and completed polymerization reaction with higher degree of cross linking.[50–52] This can explain the differences in the flexural strength and flexural modulus values between the specimens post-cured with Scheu oven with LED light source for 3 minutes only, while the specimens post-cured in a Form Cure oven were exposed to a combination of LED light source and higher temperature (60° C) for 30 minutes. This was more evident especially when the specimens were printed with 100 µm thickness layer.

The presence of a nitrogen gas atmosphere inside the Scheu oven enables the post-curing process to be carried out under inert conditions in order to overcome the detrimental effect of oxygen inhibition layer.[53,54] This might have played a role in enhancing the surface hardness values for such specimens only when printed with 50 µm layer thickness.

The subgroup III, which is the non-post-cured one, recorded the lowest significant degree of conversion and mechanical properties except the work of fracture under dry and water storage. These could be explained by the presence of a greater amount of residual unreacted monomers that causes oxidation and hydrolytic degradation, which may be manifested in the form of lower mechanical properties and accelerated wear.[55] The work of fracture was the highest for the

non-post-cured specimens and increased significantly after water storage. This phenomenon has the same explanation as mentioned before since the higher residual monomer content enhances swelling, softness of the polymer and increases the amount of water sorption. Hence, it may induce the flexibility of the material allowing more noticed bending of the specimens.[31,56] A previous study showed that the values for work of fracture for Major.Base.20 (Major) and ProBase Hot (Ivoclar-Vivadent), which are two conventional heat polymerizing denture base resins were 380 ±30 and 270 ±30 J/m^2,which is higher than the recorded values for the post-cured specimens.[57] The results of the hardness test where the same subgroup showed slightly more than 80% reduction in microhardness values after water storage were in agreement with a previous study where it was found that composite resins with the poorest degree of curing showed the most reduction in hardness after water storage.[56]

Water storage reduced the investigated mechanical properties for the tested groups which is due to the plasticizing effect of water on the polymer network and is in agreement with previous reports.[31,56,58,59] Water sorption decreases the mechanical properties of resin materials until they have been completely water-saturated within 4-6 weeks. After that, no further reduction in the mechanical properties occurs and they remain the same.[58,60]

Further analysis and investigations on physicochemical properties of this 3D printed splint material and other splint materials available in the market for 3D printing are needed such as differential scanning calorimetry (DSC) and residual monomer quantification.

Conclusions

Within the limitations of the current study the following can be concluded:

1. The post-curing method, water storage and printing layer thickness play a role in the mechanical properties of 3D printed occlusal splints.

2. The combination of heat and light within the post-curing unit can enhance the mechanical properties and degree of conversion of 3D printed occlusal splints.
3. Flexural strength and surface hardness can increase when decreasing printing layer thickness.

References

1. Dao, T. T. & Lavigne, G. J. Oral splints: the crutches for temporomandibular disorders and bruxism? *Crit. Rev. Oral Biol. Med.* **9**, 345–361 (1998).
2. Klasser, G. D. & Greene, C. S. Oral appliances in the management of temporomandibular disorders. *Oral Surg Oral Med Oral Pathol Oral Radiol Endod* **107**, 212–223 (2009).
3. Fricton, J. *et al.* Systematic review and meta-analysis of randomized controlled trials evaluating intraoral orthopedic appliances for temporomandibular disorders. *J Orofac Pain* **24**, 237–254 (2010).
4. Kuzmanovic Pficer, J. *et al.* Occlusal stabilization splint for patients with temporomandibular disorders: Meta-analysis of short and long term effects. *PLoS One* **12**, (2017).
5. Leib, A. M. Patient preference for light-cured composite bite splint compared to heat-cured acrylic bite splint. *J. Periodontol.* **72**, 1108–1112 (2001).
6. Dedem, P. & Türp, J. C. Digital Michigan splint - from intraoral scanning to plasterless manufacturing. *Int J Comput Dent* **19**, 63–76 (2016).
7. Lauren, M. & McIntyre, F. A new computer-assisted method for design and fabrication of occlusal splints. *Am J Orthod Dentofacial Orthop* **133**, S130-135 (2008).
8. Salmi, M., Paloheimo, K.-S., Tuomi, J., Ingman, T. & Mäkitie, A. A digital process for additive manufacturing of occlusal splints: a clinical pilot study. *J R Soc Interface* **10**, 20130203 (2013).
9. Berntsen, C., Kleven, M., Heian, M. & Hjortsjö, C. Clinical comparison of conventional and additive manufactured stabilization splints. *Acta Biomater Odontol Scand* **4**, 81–89 (2018).
10. Gonçalves, F. A. M. M. *et al.* The potential of unsaturated polyesters in biomedicine and tissue engineering: Synthesis, structure-properties relationships and additive manufacturing. *Progress in Polymer Science* **68**, 1–34 (2017).
11. Väyrynen, V. O. E., Tanner, J. & Vallittu, P. K. The anisotropicity of the flexural properties of an occlusal device material processed by stereolithography. *J Prosthet Dent* **116**, 811–817 (2016).
12. Berntsen, C., Kleven, M., Heian, M. & Hjortsjö, C. Clinical comparison of conventional and additive manufactured stabilization splints. *Acta Biomater Odontol Scand* **4**, 81–89 (2018).

13. Alaqeel, S. *et al.* Effect of 3D printing direction and water storage on nano-mechanical properties of 3D printed and auto-polymerized polymer with special emphasis on printing layer interface. *Materials Express* **9**, 351–357 (2019).

14. Lauren, M. & McIntyre, F. A new computer-assisted method for design and fabrication of occlusal splints. *Am J Orthod Dentofacial Orthop* **133**, S130-135 (2008).

15. Zinser, M. J., Mischkowski, R. A., Sailer, H. F. & Zöller, J. E. Computer-assisted orthognathic surgery: feasibility study using multiple CAD/CAM surgical splints. *Oral Surg Oral Med Oral Pathol Oral Radiol* **113**, 673–687 (2012).

16. Panwar, A. & Tan, L. P. Current Status of Bioinks for Micro-Extrusion-Based 3D Bioprinting. *Molecules* **21**, (2016).

17. Wickström, H. *et al.* Inkjet Printing of Drug-Loaded Mesoporous Silica Nanoparticles-A Platform for Drug Development. *Molecules* **22**, (2017).

18. Fina, F., Goyanes, A., Gaisford, S. & Basit, A. W. Selective laser sintering (SLS) 3D printing of medicines. *Int J Pharm* **529**, 285–293 (2017).

19. van Noort, R. The future of dental devices is digital. *Dent Mater* **28**, 3–12 (2012).

20. Gao, Y., Xu, L., Zhao, Y., You, Z. & Guan, Q. 3D printing preview for stereo-lithography based on photopolymerization kinetic models. *Bioact Mater* **5**, 798–807 (2020).

21. Liu, Q., Leu, M. C. & Schmitt, S. M. Rapid prototyping in dentistry: technology and application. *Int J Adv Manuf Technol* **29**, 317–335 (2006).

22. Kunjan, C., N, J. & Chandrasekhar, U. Influence of layer thickness on mechanical properties in stereolithography. *Rapid Prototyping Journal* **12**, 106–113 (2006).

23. Al Mortadi, N., Eggbeer, D., Lewis, J. & Williams, R. J. CAD/CAM/AM applications in the manufacture of dental appliances. *Am J Orthod Dentofacial Orthop* **142**, 727–733 (2012).

24. Stansbury, J. W. & Idacavage, M. J. 3D printing with polymers: Challenges among expanding options and opportunities. *Dental Materials* **32**, 54–64 (2016).

25. Rengier, F. *et al.* 3D printing based on imaging data: review of medical applications. *Int J CARS* **5**, 335–341 (2010).

26. Väyrynen, V. O. E., Tanner, J. & Vallittu, P. K. The anisotropicity of the flexural properties of an occlusal device material processed by stereolithography. *J Prosthet Dent* **116**, 811–817 (2016).

27. Huettig, F., Kustermann, A., Kuscu, E., Geis-Gerstorfer, J. & Spintzyk, S. Polishability and wear resistance of splint material for oral appliances produced with conventional, subtractive, and additive manufacturing. *Journal of the Mechanical Behavior of Biomedical Materials* **75**, 175–179 (2017).

28. Lutz, A.-M. *et al.* Fracture resistance and 2-body wear of 3-dimensional–printed occlusal devices. *The Journal of Prosthetic Dentistry* **121**, 166–172 (2019).

29. Ogliari, F. A. *et al.* Influence of chain extender length of aromatic dimethacrylates on polymer network development. *Dent Mater* **24**, 165–171 (2008).

30. Bijelic-Donova, J., Garoushi, S., Vallittu, P. K. & Lassila, L. V. J. Mechanical properties, fracture resistance, and fatigue limits of short fiber reinforced dental composite resin. *J Prosthet Dent* **115**, 95–102 (2016).

31. Bijelic-Donova, J., Garoushi, S., Lassila, L. V. J., Keulemans, F. & Vallittu, P. K. Mechanical and structural characterization of discontinuous fiber-reinforced dental resin composite. *J Dent* **52**, 70–78 (2016).

32. Perea-Lowery, L., Minja, I. K., Lassila, L., Ramakrishnaiah, R. & Vallittu, P. K. Assessment of CAD-CAM polymers for digitally fabricated complete dentures. *J Prosthet Dent* (2020) doi:10.1016/j.prosdent.2019.12.008.

33. Schulte, J. K., Anderson, G. C., Sakaguchi, R. L. & DeLong, R. Wear resistance of isosit and polymethyl methacrylate occlusal splint material. *Dent Mater* **3**, 82–84 (1987).

34. Steyrer, B., Neubauer, P., Liska, R. & Stampfl, J. Visible Light Photoinitiator for 3D-Printing of Tough Methacrylate Resins. *Materials (Basel)* **10**, (2017).

35. Karalekas, D. & Aggelopoulos, A. Study of shrinkage strains in a stereolithography cured acrylic photopolymer resin. *Journal of Materials Processing Technology* **136**, 146–150 (2003).

36. Hague, R., Mansour, S., Saleh, N. & Harris, R. Materials analysis of stereolithography resins for use in Rapid Manufacturing. *Journal of Materials Science* **39**, 2457–2464 (2004).

37. Nishigawa, K., Bando, E. & Nakano, M. Quantitative study of bite force during sleep associated bruxism. *Journal of Oral Rehabilitation* **28**, 485–491 (2001).

38. Choudhary, S. & Suprabha, B. S. Effectiveness of light emitting diode and halogen light curing units for curing microhybrid and nanocomposites. *Journal of Conservative Dentistry* **16**, 233 (2013).

39. Torno, V. *et al.* Effects of irradiance, wavelength, and thermal emission of different light curing units on the Knoop and Vickers hardness of a composite resin. *J. Biomed. Mater. Res. Part B Appl. Biomater.* **85**, 166–171 (2008).

40. Dionysopoulos, D., Papadopoulos, C. & Koliniotou-Koumpia, E. Effect of temperature, curing time, and filler composition on surface microhardness of composite resins. *J Conserv Dent* **18**, 114–118 (2015).

41. O'Neill, P. F., Kent, N. & Brabazon, D. Mitigation and control of the overcuring effect in mask projection micro-stereolithography. in (2017). doi:10.1063/1.5008249.

42. Choi, J., Wicker, R. B., Cho, S., Ha, C. & Lee, S. Cure depth control for complex 3D microstructure fabrication in dynamic mask projection microstereolithography. *Rapid Prototyping Journal* **15**, 59–70 (2009).

43. Lemon, M. T., Jones, M. S. & Stansbury, J. W. Hydrogen bonding interactions in methacrylate monomers and polymers. *J Biomed Mater Res A* **83**, 734–746 (2007).

44. Hubbezoglu, I. *et al.* Microhardness Evaluation of Resin Composites Polymerized by Three Different Light Sources. *Dental Materials Journal* **26**, 845–853 (2007).

45. Kurachi, C., Tuboy, A. M., Magalhães, D. V. & Bagnato, V. S. Hardness evaluation of a dental composite polymerized with experimental LED-based devices. *Dental Materials* **17**, 309–315 (2001).

46. Yoon, T.-H., Lee, Y.-K., Lim, B.-S. & Kim, C.-W. Degree of polymerization of resin composites by different light sources. *Journal of Oral Rehabilitation* **29**, 1165–1173 (2002).

47. Franz, A., König, F., Lucas, T., Watts, D. C. & Schedle, A. Cytotoxic effects of dental bonding substances as a function of degree of conversion. *Dent Mater* **25**, 232–239 (2009).

48. Durner, J., Obermaier, J., Draenert, M. & Ilie, N. Correlation of the degree of conversion with the amount of elutable substances in nano-hybrid dental composites. *Dent Mater* **28**, 1146–1153 (2012).

49. Calheiros, F. C., Daronch, M., Rueggeberg, F. A. & Braga, R. R. Degree of conversion and mechanical properties of a BisGMA:TEGDMA composite as a function of the applied radiant exposure. *J. Biomed. Mater. Res. Part B Appl. Biomater.* **84**, 503–509 (2008).

50. Daronch, M., Rueggeberg, F. A. & De Goes, M. F. Monomer conversion of pre-heated composite. *J. Dent. Res.* **84**, 663–667 (2005).

51. Park, S. H. & Lee, C. S. The difference in degree of conversion between light-cured and additional heat-cured composites. *Oper Dent* **21**, 213–217 (1996).

52. Ahn, K. H., Lim, S., Kum, K. Y. & Chang, S. W. Effect of preheating on the viscoelastic properties of dental composite under different deformation conditions. *Dental Materials Journal* **34**, 702–706 (2015).

53. Bijelic-Donova, J., Garoushi, S., Lassila, L. V. J. & Vallittu, P. K. Oxygen inhibition layer of composite resins: effects of layer thickness and surface layer treatment on the interlayer bond strength. *Eur. J. Oral Sci.* **123**, 53–60 (2015).

54. Sehgal, A., Rao, Y. M., Joshua, M. & Narayanan, L. L. Evaluation of the effects of the oxygen-inhibited layer on shear bond strength of two resin composites. *J Conserv Dent* **11**, 159–161 (2008).

55. Sideridou, I. D. & Achilias, D. S. Elution study of unreacted Bis-GMA, TEGDMA, UDMA, and Bis-EMA from light-cured dental resins and resin composites using HPLC. *J. Biomed. Mater. Res. Part B Appl. Biomater.* **74**, 617–626 (2005).

56. Ferracane, J. L., Berge, H. X. & Condon, J. R. In vitro aging of dental composites in water—Effect of degree of conversion, filler volume, and filler/matrix coupling. *Journal of Biomedical Materials Research* **42**, 465–472 (1998).

57. Stafford, G. D., Huggett, R. & Causton, B. E. Fracture toughness of denture base acrylics. *J. Biomed. Mater. Res.* **14**, 359–371 (1980).

58. Ferracane, J. L. & Marker, V. A. Solvent Degradation and Reduced Fracture Toughness in Aged Composites. *J Dent Res* **71**, 13–19 (1992).

59. Medeiros, I. S., Gomes, M. N., Loguercio, A. D. & Filho, L. E. R. Diametral tensile strength and Vickers hardness of a composite after storage in different solutions. *Journal of Oral Science* **49**, 61–66 (2007).

60. Lassila, L. V. J., Nohrström, T. & Vallittu, P. K. The influence of short-term water storage on the flexural properties of unidirectional glass fiber-reinforced composites. *Biomaterials* **23**, 2221–2229 (2002).